Protein kinase C promotes choline transporter-like protein 1 function via improved cell surface expression in immortalized human hepatic cells

TAKUYA ISHIKAWA[1], HIROTSUGU SUWANAI[1], JUNPEI SHIKUMA[1], RYO SUZUKI[1], TSUYOSHI YAMANAKA[2], MASATO ODAWARA[1] and MASATO INAZU[2,3]

[1]Department of Diabetes, Metabolism and Endocrinology, Tokyo Medical University, Tokyo 160-0023; [2]Department of Molecular Preventive Medicine, Tokyo Medical University; [3]Institute of Medical Science, Tokyo Medical University, Tokyo 160-8402, Japan

Received July 6, 2019; Accepted October 16, 2019

DOI: 10.3892/mmr.2019.10894

Abstract. Choline is used to synthesize phospholipids and a lack of choline induces a number of liver-related diseases, including non-alcoholic steatohepatitis. The current study characterized the choline uptake system, at molecular and functional levels, in the immortalized human hepatic cell line, Fa2N-4, to identify the specific choline transporter involved in choline uptake. The present study also assesed whether choline deficiency or the inhibited choline uptake affected cell viability and apoptosis. Reverse transcription-quantitative polymerase chain reaction (PCR) revealed choline transporter-like protein 1 (CTL1) and CTL2 mRNA and protein expression in Fa2N-4 cells. [Methyl-^{3}H]choline studies revealed choline uptake was saturable and mediated by a single transport system that functioned in a Na^+-independent but pH-dependent manner, which was similar to CTL1. Hemicholinium-3 (HC-3), which is a choline uptake inhibitor, and choline deficiency inhibited cell viability, increased caspase-3 and -7 activities, and increased fluorescein isothiocyanate-Annexin V immunofluorescent staining indicated apoptosis. Immunofluorescent staining also revealed CTL1 and CTL2 localized in plasma and mitochondrial membranes, respectively. [Methyl-^{3}H]choline uptake was enhanced by a protein kinase C (PKC) activator, phorbol-12-myristate 13-acetate (PMA). Immunofluorescence staining and western blot analysis demonstrated increased CTL1 expression on the cell membrane following PMA treatment. The results of current study indicated that extracellular choline is primarily transported via CTL1, relying on a direct H^+ gradient that functions as a driving force in Fa2N-4 cells. Furthermore, it was hypothesized that CTL1 and the choline uptake system are strongly associated with cell survival, and that the choline uptake system is modulated by PKC signaling via increased CTL1 expression on the cell surface. These findings provide further insights into the pathogenesis of liver disease involving choline metabolism.

Introduction

Choline is a water-soluble and vitamin-like nutrient. In humans, cellular absorption of choline occurs via choline transporters. It is subsequently metabolized and used for various functions, such as in the regulation of osmotic pressure, as a methyl donor precursor in epigenetics, and for phospholipid synthesis. Choline metabolism is divided into three major pathways: i) Acetylation, ii) phosphorylation, and iii) oxidation, which are associated with the synthesis of acetylcholine, phosphatidylcholine (PC), and methyl group donors, respectively. To date, three major choline transporters have been identified (1). The high-affinity choline transporter, CHT1/SLC5A7, is believed to be unique to cholinergic neurons (2). Second, polyspecific organic cation transporters (OCT1-3/SLC22A1-3) exhibit a low affinity toward choline (3). Lastly, choline transporter-like proteins (CTL1-5/SLC44A1-5) are present in various human tissues (4). Previous reports have demonstrated that CTL1 is often functionally expressed on the cell membrane and is responsible for extracellular choline transportation (1,5). However, modulation of the choline uptake system in human homeostasis as well as the signaling pathways involved remain unclear. Protein kinase C (PKC) regulates the expression of various transporters on the cell surface, such as gamma-aminobutyric acid, serotonin, and dopamine transporters (6). PKC signaling is also reportedly associated with the repression of choline uptake in differentiated monocytes (7). Choline metabolism depends on the cellular environment, by which it

Correspondence to: Professor Masato Inazu, Institute of Medical Science, Tokyo Medical University, 6-1-1 Shinjuku, Shinjuku-ku, Tokyo 160-8402, Japan
E-mail: inazu@tokyo-med.ac.jp

Abbreviations: GAPDH, glyceraldehyde-3-phosphate dehydrogenase; HCC, hepatocellular carcinoma; NAFLD, non-alcoholic fatty liver disease; NASH, non-alcoholic steatohepatitis; PCR, polymerase chain reaction; PMA, phorbol 12-myristate 13-acetate; 4α-PMA, 4α-phorbol 12-myristate 13-acetate; PC, phosphatidylcholine

Key words: choline, choline transporter, hepatocytes, membrane transport proteins, protein kinase C, choline deficiency

proceeds via various available metabolic pathways. Previous studies have revealed a major role played by the liver in choline metabolism (8). The liver is the major PC-metabolizing organ; therefore, it is strongly associated with choline metabolism (9), highlighting the considerable demand for choline by the liver for its optimal functioning. This suggests that hepatic cell function is at least partly modulated via PKC signaling. The liver cannot participate in the active synthesis of phospholipids without choline; thus, a choline shortage induces various liver-related diseases (10-12). A better understanding of the relationship between the liver, choline, and choline metabolites may lead to an improved understanding of the pathogenesis of various liver-related diseases. However, the relationship between the liver, choline uptake system and functional expression of choline transporters expressed on hepatic cells remains to be clarified. Therefore, we undertook structural, functional, and molecular analyses of the choline uptake system in the human immortalized hepatic cell line, Fa2N-4. Furthermore, we examined whether choline-deficient conditions and the inhibition of choline uptake affected cell viability, and caspase-3 and -7 activities. In addition, we investigated whether treatment of Fa2N-4 cells with a known PKC activator, phorbol-12-myristate 13-acetate (PMA), affected modulation of the choline uptake system.

Materials and methods

Cell culture. The immortalized human hepatic cell line, Fa2N-4, was acquired from Sekisui XenoTech LLC and cultured in RPMI 1640 medium supplemented with 10% fetal bovine serum (Gibco; Thermo Fisher Scientific, Inc.) and 20 mg/l kanamycin (Gibco; Thermo Fisher Scientific, Inc.) in collagen-coated flasks. The flasks were kept in an atmosphere comprising 5% CO_2 and 95% air at 37˚C. The culture medium was replaced every 2-3 days.

[Methyl-^{3}H]choline uptake by Fa2N-4 cells. [Methyl-^{3}H]choline chloride (specific activity: 3182 GBq/mmol) was acquired from PerkinElmer Life Sciences, Inc.. A DC protein assay kit was acquired from Bio-Rad Laboratories. PMA and 4α-phorbol 12-myristate 13-acetate (4α-PMA) were acquired from Wako Pure Chemical Industries, Ltd., and hemicholinium-3 (HC-3) was obtained from Sigma-Aldrich, Merck KGaA. We assessed the properties of [methyl-^{3}H]choline chloride uptake according to a previous study (13). Radioactivity was measured using a liquid scintillation counter (Tri-Carb® 2100TR, Packard) and [methyl-^{3}H]choline specific uptake was calculated as the difference between total [methyl-^{3}H]choline uptake in the presence and absence of 30 mM of unlabeled choline. Protein concentrations were determined using a DC protein assay kit according to the manufacturer's instructions.

RNA extraction and real-time polymerase chain reaction assay. The cells were first washed using Dulbecco's phosphate buffered saline (D-PBS). Total RNA was extracted from the cells using a QIAshredder and RNeasy Mini kit (Qiagen Inc.) according to the manufacturer's instructions. TaqMan probes for target mRNAs (CHT1, OCT1-3, CTL1-5, and the housekeeping gene, glyceraldehyde-3-phosphate dehydrogenase [*GAPDH*]) were designed based on its human mRNA sequence using TaqMan® Gene Expression Assays (Applied Biosystems; Thermo Fisher Scientific, Inc.). Detailed information on primers for real-time polymerase chain reaction (PCR) assays is outlined in Table I. Since the sequences related to the primers and probes of the TaqMan® Gene Expression Assay are not disclosed, the assay ID is shown in Table I. For one-step real-time PCR, 50 ng total RNA was added to a master mix using a TaqMan® RNA-to-CT™ 1-Step kit (Applied Biosystems; Thermo Fisher Scientific, Inc.) according to the manufacturer's instructions. Next, real-time PCR analysis was conducted using a StepOne Plus™ Real-Time PCR system (Applied Biosystems; Thermo Fisher Scientific, Inc.). Relative levels of the mRNAs of target genes were determined using a comparative cycle time (Ct) method, whereas levels of mRNA expression relative to *GAPDH* for each target PCR were determined as follows: Relative mRNA expression = $2^{-(Ct\ target\ -\ Ct\ GAPDH)}$ x 100%.

Immunoblotting. A RIPA lysis buffer system (sc-24948) and β-ME Sample Treatment for Tris-SDS were acquired from Santa Cruz Biotechnology, Inc. and Cosmo Bio Corporation, respectively. Protein Multicolor III was acquired from BioDynamics Laboratory Inc.. A Mini-PROTEAN® TGX™ Gel and Trans-Blot® Turbo™ Transfer Pack were acquired from Bio-Rad Laboratories, Inc. Anti-CTL1 polyclonal antibody (ab110767), anti-NaK-ATPase monoclonal antibody (ab76020) as an internal control for the cell membrane, and anti-cytochrome *c* oxidase (COX) IV antibody (ab16056) were acquired from Abcam. Anti-CTL2 monoclonal antibody (clone 3D11) was obtained from Abnova Corporation. Anti-β-actin pAb-HRP-DirecT antibody (PM053-7) was obtained from MBL. Fa2N-4 cell culture was performed according to a previously published procedure (13). In brief, membranes were incubated with rabbit anti-CTL1 polyclonal (ab110767) and anti-CTL2 monoclonal (clone 3D11) antibodies. Protein bands were separated by SDS-polyacrylamide gel electrophoresis, blotted onto a PVDF membrane and visualized using an ECL Prime Western Blotting Detection system (GE Healthcare Life Sciences). Luminescent images were acquired using a ChemiDoc XRS Plus system (Bio-Rad Laboratories, Inc.). A Mitochondria/Cytosol Fractionation kit (ab65320) was acquired from Abcam plc and used to isolate proteins from the mitochondrial fraction. A Trident Membrane Protein Extraction kit (Genetex, Inc.) was used to obtain proteins from the membrane fraction.

Immunofluorescence staining. Wash solution, detector blocking solution, and horseradish peroxidase-conjugated anti-rabbit and anti-mouse IgG were acquired from Kirkegaard and Perry Laboratories Inc. Vectashield mounting medium containing 4',6-diamidino-2-phenylindole (DAPI) was acquired from Vector Laboratories, Inc.. In addition, Alexa Fluor 488 goat anti-rabbit, anti-mouse IgG, 568 goat anti-rabbit, and anti-mouse IgG were acquired from Molecular Probes Inc. Fa2N-4 cells cultured on a 35-mm glass base dish (Iwaki Glass Co.) were washed twice with D-PBS and fixed with 100% methanol for 20 min at room temperature. Consequently, the cells were treated with iBind Flex Solution (Thermo Fisher Scientific, Inc.) for 1 h. Co-localization of CTL1 with the cell membrane was examined using a NaK-ATPase antibody and that of CTL2 within

Table I. TaqMan® gene expression assay.

Gene	Accession number	Assay ID	Exon boundary	Assay location	Amplicon length
CHT1 (SLC5A7)	NM_021815	Hs00222367_m1	4-5	749	66
CTL1 (SLC44A1)	NM_080546	Hs00223114_m1	5-6	759	66
CTL2 (SLC44A2)	NM_020428	Hs01105936_m1	20-21	2,060	67
CTL3 (SLC44A3)	NM_001114106	Hs00537043_m1	5-6	625	64
CTL4 (SLC44A4)	NM_001178044	Hs00228901_m1	12-13	1,177	58
CTL5 (SLC44A5)	NM_152697	Hs01120485_m1	9-10	673	73
OCT1 (SLC22A1)	NM_003057	Hs00427554_m1	8-9	1,493	66
OCT2 (SLC22A2)	NM_003058	Hs01010723_m1	10-11	1,771	120
OCT3 (SLC22A3)	NM_021977	Hs01009568_m1	10-11	1,657	73
GAPDH	NM_002046	Hs99999905_m1	3-3	243	122

the mitochondrial membrane using a mitochondrial marker, COX IV antibody. Antibody staining was performed according to a previously published protocol (13). Immunofluorescence images were obtained using a confocal laser scanning microscope FV10i-DOC (Olympus).

Cell viability assay. Choline chloride, and RPMI 1640 medium, with and without choline chloride were acquired from Wako Pure Chemical Industries, Ltd. Fa2N-4 cells were plated at a density of $5x10^4$ cells/well in 24-well plates. Inhibitors were added 24 h after cell plating, and the final volume of the medium in each well was maintained at 1.0 ml. Cell numbers were measured using an ATPLite™ luminescence ATP detection assay system (PerkinElmer Life and Analytical Sciences) according to the manufacturer's instructions. A FilterMax F5 Multi-Mode Microplate Reader was used to measure luminescence (Molecular Devices, LLC).

Measurement of caspase-3 and -7 activities. Caspase-3 and -7 activities were measured using a Caspase-Glo® 3/7 Assay kit (Promega Corporation) according to the manufacturer's instructions. In brief, this kit is based on cleavage of the DEVD sequence of a luminogenic substrate by caspase-3 and -7, emitting a luminescence signal. Fa2N-4 cells were seeded at a density of $5x10^4$ cells/well in 24-well plates. HC-3 was added or choline-deficient medium was replaced after cell plating for 24 h. Each well had a final volume of 1.0 ml medium. Caspase-3 and -7 activities were measured after the addition of HC-3 or replacement of choline-deficient medium using a Caspase-Glo®3/7 Assay kit. A FilterMax F5 Multi-Mode Microplate Reader was used to measure luminescence.

Apoptotic/necrotic/healthy cell detection assay. Apoptotic, necrotic, and healthy cells were detected using an apoptotic/necrotic/healthy cell detection kit (Promocell) according to the manufacturer's instructions. Briefly, cells were initially seeded and cultured at 80 to 90% confluency. For experiments, cells were cultured in defined RPMI-1640 with normal saline for 48 and 72 h as a control, without choline chloride (choline deficiency: CD) for 48 h, or with 1 mM of HC-3 (HC-3) for 72 h, and then stained with Hoechst 33342 (blue, nucleus), fluorescein isothiocyanate (FITC)-Annexin V (green) and ethidium homodimer III (EthD-III; red) for 15 min. A Confocal Laser Scanning Biological Microscope (FV10i-DOC; Olympus) was used to acquire fluorescent images.

Statistical analysis. Data are presented as mean ± standard deviation (SD). Statistical analyses were conducted using Dunnett's multiple comparison test and unpaired t-test using GraphPad Prism 8 software (GraphPad Software, Inc.). Statistical significance was assigned for P-values <0.05. GraphPad Prism 6 was used to calculate kinetic parameters with Michaelis-Menten kinetics. We also applied saturation (hyperbola) kinetics to the values. K_i values were derived using $K_i = IC_{50}/[1 + (L)/K_m]$, where (L) represents the radiolabeled ligand concentration from half maximal inhibitory concentration (IC_{50}) values as previously described (14).

Results

Choline transporter mRNA and protein in Fa2N-4 cells. CHT1, CTL1-5, and OCT1-3 mRNA levels were examined using real-time PCR. CTL1 and CTL2 mRNAs were expressed at higher levels, whereas those of CHT1, CTL4, CTL5, OCT1, and OCT2 were expressed below measurable limits in Fa2N-4 cells. Furthermore, CTL3 and OCT3 mRNAs were expressed at low levels (Fig. 1A). Both CTL1 and CTL2 expression was subsequently measured at the protein level using western blot analysis. Immunoblotting with CTL1 and CTL2 antibodies revealed bands corresponding to 70 and 60 kDa, respectively (Fig. 1B). The subcellular distribution of CTL1 and CTL2 in Fa2N-4 cells was determined using immunofluorescence staining. CTL1 immunoreactivity was predominantly identified on the cell surface and overlapped with the cell surface marker, NaK-ATPase (Fig. 1C). In contrast, CTL2 immunoreactivity was identified in intracellular compartments and overlapped with that of COX IV, a mitochondrial marker (Fig. 1C). Thus CTL1 and CTL2 mRNA and protein were expressed in Fa2N-4 cells, with CTL1 localized to the cell surface and CTL2 localized in mitochondria.

[Methyl-^{3}H]choline uptake in Fa2N-4 cells. We next examined the time course of [methyl-^{3}H]choline uptake in Fa2N-4 cells at a concentration of 10 μM in the presence and absence of

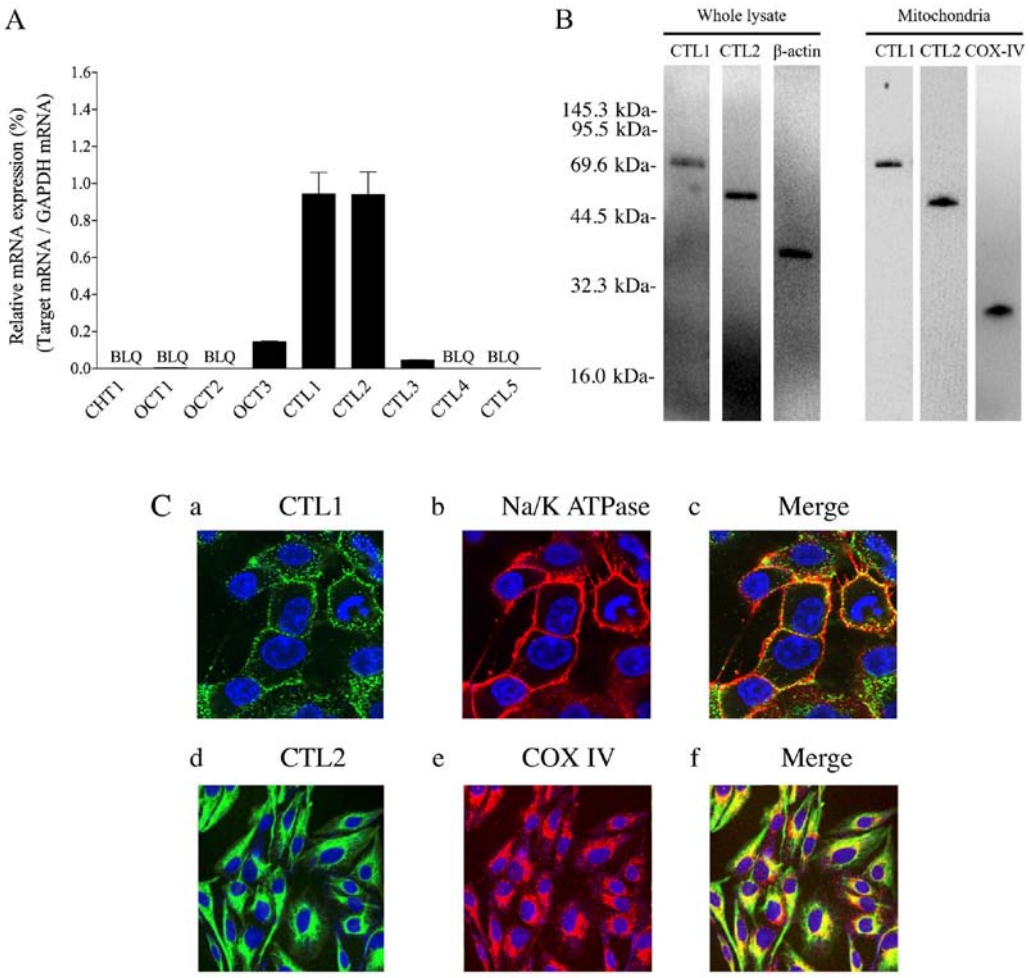

Figure 1. CTL1 and CTL2 mRNA and protein expression in Fa2N-4 cells. (A) Relative mRNA expression is presented as a ratio of target mRNA to GAPDH mRNA (n=3). Each column represents mean ± standard deviation. BLQ indicates values below the limit of quantification. (B) Fa2N-4 whole cell and mitochondrial lysates were used. With a whole cell protein lysate, choline transporter-like protein 1 (CTL1), CTL2 and β-actin proteins were detected, whereas CTL1, CTL2, and COX-IV proteins were detected within mitochondrial lysate. (C) Localization of CTL1 and CTL2 proteins in Fa2N-4 cells were analyzed using the cell membrane and mitochondrial markers, NaK-ATPase and COX IV, respectively. The presence of CTL1 is indicated by a green signal (a), and a merged image of CTL1 and NaK-ATPase (b) is presented in panel (c). The presence of CTL2 is represented a green signal (d), and merged images of CTL2 and COX IV (e) are shown in panel (f). 4',6-diamidino-2-phenylindole (DAPI)-stained nuclei are shown as blue signals in each panel. Images in (a-c) have a magnification, x120 whereas (d and e) have a magnification, x60. CTL, choline transporter-like protein; COX-IV, cytochrome *c* oxidase; BLQ, below the limit of quantification.

extracellular Na^+. [Methyl-^{3}H]choline uptake linearly increased in a time-dependent manner for at least 20 min (Fig. 2A). Upon the replacement of NaCl with N-methyl-D-glucamine chloride (NMDG-Cl) in the uptake buffer, [methyl-^{3}H]choline uptake increased under Na^+-free conditions compared with that of the control under normal conditions (Fig. 2A). The kinetic analysis of [methyl-^{3}H]choline uptake computed by saturation kinetics analysis generated a Michaelis-Menten constant (K_m) of 8.0±0.1 μM and maximal velocity (V_{max}) of 2,100±107.1 pmol/mg protein/h (Fig. 2B). We also applied saturation (hyperbola) kinetics to the values; however, the respective K_m and V_{max} were the same. An Eadie-Hofstee plot showed a single process in [methyl-^{3}H]choline uptake based on linear regression analysis (Fig. 2B). The effect of extracellular pH on [methyl-^{3}H]choline uptake in Fa2N-4 cells was examined by varying the pre-incubation medium pH between 6.0 and 8.5. [Methyl-^{3}H]choline uptake was significantly decreased and increased when extracellular pH was reduced from 7.5 to 6.0 and increased from 7.5 to 8.5, respectively (Fig. 2C). Furthermore, the effect of HC-3, an inhibitor of choline uptake, on [methyl-^{3}H]choline uptake in Fa2N-4 cells was examined. It was observed that the uptake was inhibited by HC-3 in a concentration-dependent manner, with a K_i value of 48.2 μM (Fig. 2D). Thus, [methyl-^{3}H]choline uptake by Fa2N-4 cells increased in a time-and pH-dependent manner, and was increased in the absence of Na^+ and inhibited by HC-3.

Choline deficiency and HC-3 decreased cell viability, increased caspase-3 and -7 activities, and induced apoptotic change in Fa2N-4 cells. The effect of choline deficiency and 1 mM HC-3 treatment on caspase-3 and -7 activities in Fa2N-4 cells was evaluated. It was observed that HC-3 treatment and choline deficiency significantly inhibited cell viability and increased caspase-3 and -7 activities in these cells (Fig. 3A). We further examined whether cell death by choline deficiency and treatment with HC-3 occurs through apoptosis or necrosis (Fig. 3B). In this experiment, immune cells were stained by Hoechst 33342 (blue, nuclei) only, and not by FITC-Annexin V

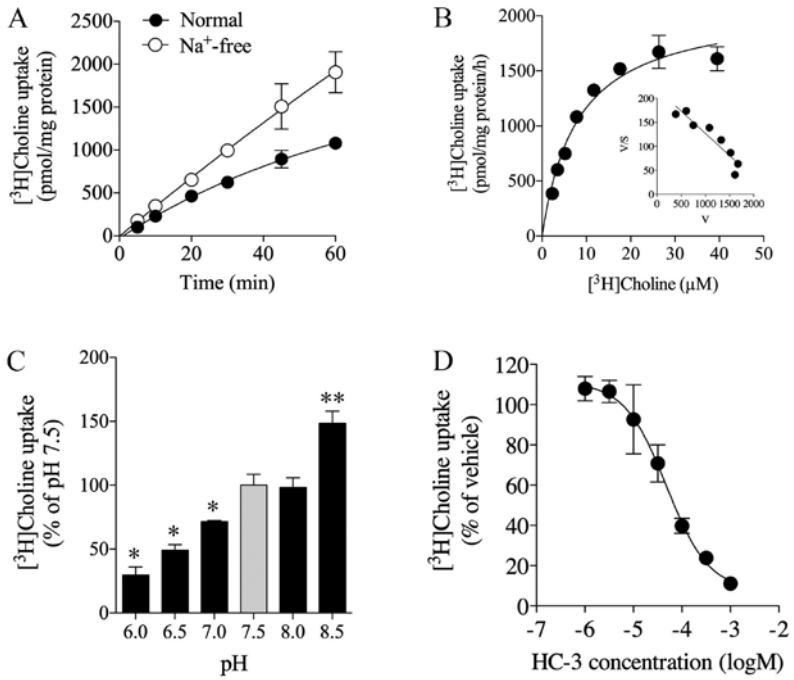

Figure 2. [Methyl-^{3}H]choline uptake in Fa2N-4 cells. (A) Time course of 10 μM [methyl-^{3}H]choline uptake in the presence and absence of extracellular Na^+ for 60 min. The assay was performed at pH 7.4 and 37˚C. Each point represents the mean ± SD (n=3). The time course of [methyl-^{3}H]choline uptake was fitted to experimental data using non-linear regression analysis. (B) Kinetic characteristics of [methyl-^{3}H]choline uptake in Fa2N-4 cells. The specific uptake of [methyl-^{3}H]choline was saturable with a K_m value of 8.0±0.1 μM and V_{max} of 2,100±107.1 pmol/mg protein/h. Inset, Eadie-Hofstee plots of [methyl-^{3}H]choline uptake shows a single straight line. Each point represents mean ± SD (n=3). (C) Influence of extracellular pH on [methyl-^{3}H]choline uptake in Fa2N-4 cells. The uptake of 10 μM [methyl-^{3}H]choline was measured for 20 min under various pH conditions. Each point represents mean ± SD (n=3). *P<0.05 and **P<0.01 compared with pH 7.5. Effects of HC-3 on [methyl-^{3}H]choline uptake in Fa2N-4 cells are presented in (D). Cells were pre-incubated with a number of HC-3 concentrations for 20 min, and the uptake of 10 μM [methyl-^{3}H]choline was measured for 20 min. The K_i value of HC-3 for the inhibition of [methyl-^{3}H]choline uptake was 48.2 μM. Each point represents mean ± SD (n=3). SD, standard deviation; HC-3, hemicholinium-3.

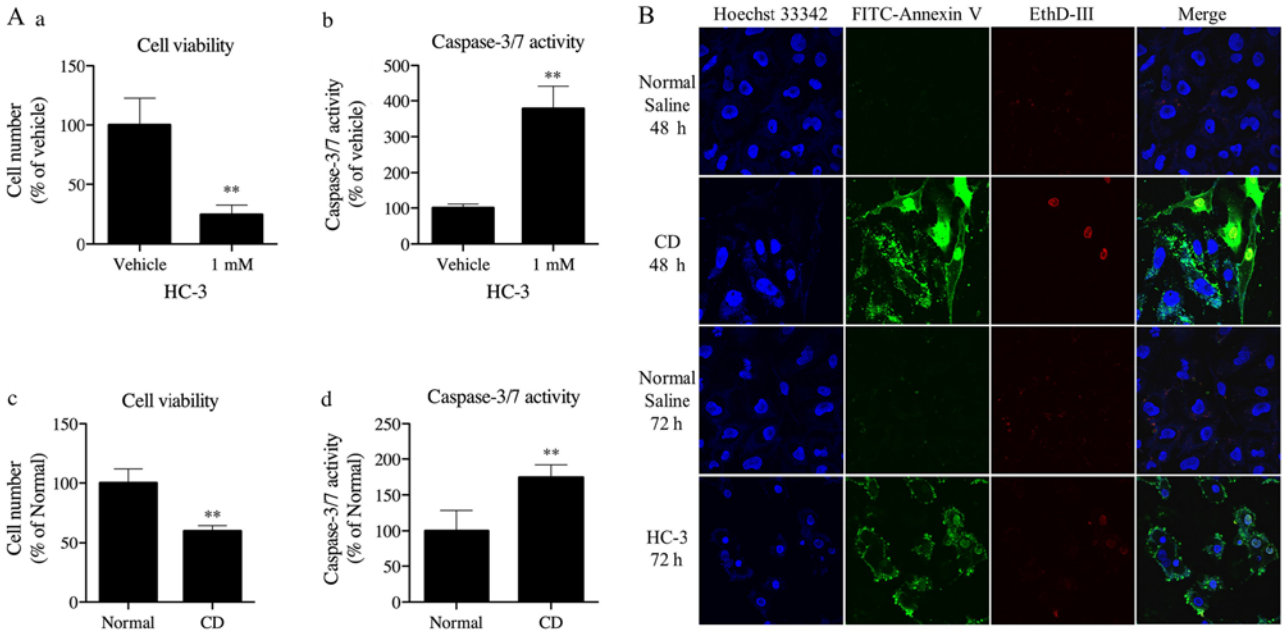

Figure 3. (A) Effect of HC-3 and choline deficiency on cell viability and caspase-3 and -7 activities in Fa2N-4 cells. (a) Treatment of Fa2N-4 cells with 1 mM HC-3 significantly inhibited cell viability and (b) significantly increased caspase-3 and -7 activities. (c) Fa2N-4 cells were cultured in RPMI 1640 medium with (normal) or without 30 μM choline chloride (CD). CD treatment significantly inhibited cell viability and (d) increased caspase-3 and -7 activities in Fa2N-4 cells. Each value represents mean ± standard deviation. (A and B, n=4; C and D, n=6). **P<0.01 compared with the vehicle or normal group. (B) Choline deficiency and HC-3 treatment induced apoptosis in Fa2N-4 cells. Cells were initially seeded and cultured at 80 to 90% confluency, and then in defined RPMI-1640 with normal saline for 48 and 72 h as a control, without choline chloride (CD) for 48 h, or with 1 mM of HC-3 (HC-3) for 72 h. Cells were stained with Hoechst 33342 (blue, nucleus), FITC-Annexin V (green) and ethidium homodimer V (EthD-V, red) for 15 min. Immune cells were stained using Hoechst 33342 (blue, nuclei), and not by FITC-Annexin V (green) or EthD-V (red). Early apoptotic cells were stained blue and green, whereas necrotic cells were stained blue and red. Cells stained blue, green and red represented dead cells progressing from an apoptotic cell change (late apoptotic cells), or necrotic cell change. Magnification, x60. HS-3, hemicholinium-3; CD, choline-deficient.

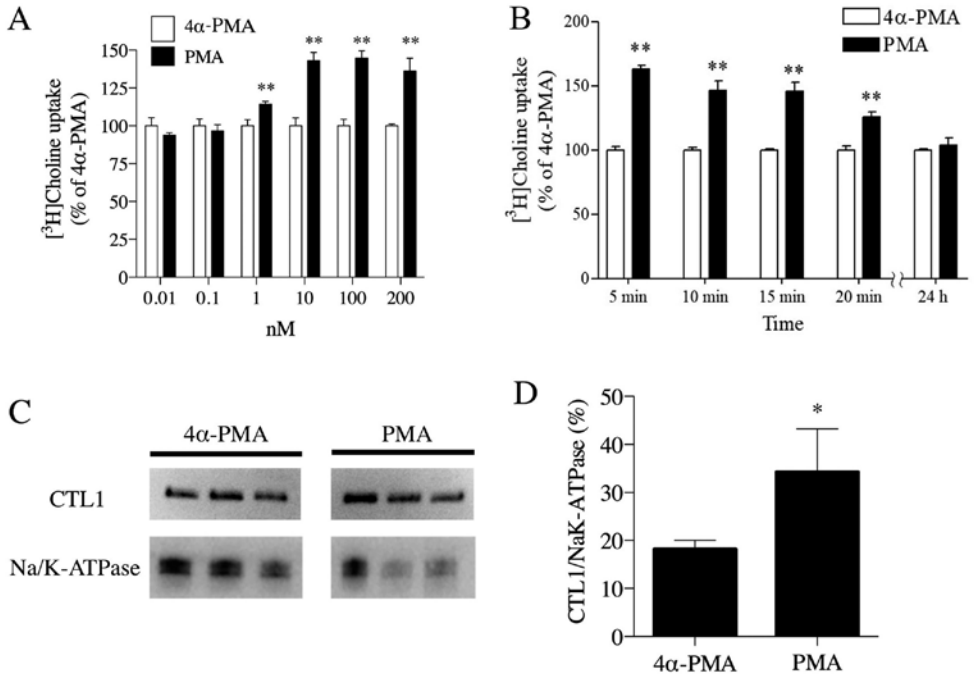

Figure 4. PKC stimulation of choline uptake and CTL1 protein in Fa2N-4 cells. (A) Fa2N-4 cells were pre-incubated with various concentrations of PMA or 4α-PMA (negative control) for 10 min and the uptake of 10 μM [methyl-^{3}H]choline measured for 20 min. Compared with the negative control, PMA treatment at increasing concentrations (1-200 nM) increased [methyl-^{3}H]choline uptake. A PMA concentration of 100 nM was optimal and led to the highest [methyl-^{3}H] choline uptake. Each point represents mean ± SD (n=3). **P<0.01 compared with 4α-PMA. (B) Fa2N-4 cells were pre-incubated with 100 nM PMA or 4α-PMA for various times, and the uptake of 10 μM [methyl-^{3}H] choline was measured for 20 min for the acute phase, and 24 h for the chronic phase. [Methyl-^{3}H]choline uptake was highest at 5 min after PMA treatment. Each point represents mean ± SD (n=3). **P<0.01 compared with the 4α-PMA control. (C) Western blot analysis was performed following stimulation of Fa2N-4 cells with 4α-PMA and PMA for 25 min. The protein components of cell membranes were extracted by a Trident Membrane Protein Extraction Kit and then used to detect CTL1 expression levels by western blot analysis. (D) Results were standardized using NaK-ATPase protein band levels. PMA stimulation resulted in a higher CTL1/NaK-ATPase protein ratio compared with the 4α-PMA stimulation group. Each point represents mean ± SD (n=3). *P<0.05 compared with the 4α-PMA stimulation group. PKC, protein kinase C; CTL, choline transporter-like protein; PMA, phorbol 12-myristate 13-acetate; SD, standard deviation.

(green) or EthD-III (red) as observed in normal saline treated cells, after 48 and 72 h. Early apoptotic cells were stained both blue and green, whereas necrotic cells were stained blue and red. Cells that stained blue, green and red represented dead cells progressing from an apoptotic cell change (late apoptotic cells), or necrotic cell change. In Fig. 3B, choline deficiency and 1 mM HC-3 treatment induced marked changes as shown by blue and green staining, which was interpreted as an apoptotic change. Thus, HC-3 treatment and choline deficiency significantly inhibited cell viability, increased caspase-3 and -7 activities and induced apoptosis in Fa2N-4 cells.

PKC stimulation of the choline transport system and CTL1. Compared with the 4α-PMA negative control, PMA treatment increased [methyl-^{3}H]choline uptake in Fa2N-4 cells. The highest uptake of [methyl-^{3}H]choline occurred when PMA was used at a concentration of 100 nM (Fig. 4A). Using 100 nM as the optimal concentration of PMA, the time course of choline uptake was analyzed, with the highest uptake of [methyl-^{3}H] choline occurring 5 min after PMA treatment (Fig. 4B). However, chronic treatment (24 h) with PMA did not increase or decrease choline uptake compared with 4α-PMA. Following stimulation by PMA, an activator of PKC, and using 4α-PMA as a negative control, cell membrane protein components were extracted using a Trident Membrane Protein Extraction kit. The extracted proteins were electrophoresed and underwent western blot analysis to detect CTL1 (Fig. 4C). The band intensities were quantified and the relative expression levels of CTL1 were standardized using NaK-ATPase. PMA-treated cells were found to have a significantly higher CTL1 band intensity than 4α-PMA-treated cells (Fig. 4D). Thus, PKC activation induced [methyl-^{3}H]choline uptake in Fa2N-4 cells and increased CTL1 in cell membranes.

Discussion

The analysis of choline transporter expression in Fa2N-4 cells indicated the high expression of CTL1 and CTL2 mRNAs, and negligible or low expression of CTL3 and OCT3 mRNAs. Functionally, a single choline transportation system, which operates independently of Na^+, is responsible for choline uptake in Fa2N-4 cells. The K_m value of choline chloride for the choline transporter was 8.0±0.1 μM, which is within the choline concentration range in the human liver (5-30 μM) (15), whereas the K_i value using HC-3 was 48.2 μM. CTL1 functions in a pH- and membrane potential-dependent manner, can operate independently of Na^+, is sensitive to organic cations, and has a proven affinity for choline (K_m value of 10-30 μM) and HC-3 (K_i> 10 μM). These characteristics of CTL1 overlap with the results of the current study. In contrast, because CHT1 operates in a Na^+-dependent manner toward choline transportation and is inhibited by HC-3 at very low concentrations (K_i value, 50-100 nM) (16), CHT1 mRNA is expressed below quantifiable levels in Fa2N-4 cells; this does

not support the concept of CHT1 predominantly contributing to the choline transport system of Fa2N-4 cells. Furthermore, choline transportation by OCTs is known to be independent of Na^+ ions. OCT1 and OCT2 have K_m values of 620 and 210 μM, respectively, whereas OCT3 does not recognize choline as a substrate (17,18). These results do not support the theory that OCTs play a predominant role in choline transportation in Fa2N-4 cells.

To date, it has been suggested that a CTL1-mediated choline uptake system functions in primary human tumor cell cultures, such as colon carcinoma cells (19), keratinocytes (20), esophageal cancer cells (21), small cell lung carcinoma cells (22), tongue cancer cells (13), and trophoblastic cells (23). Likewise, CTL1 is ubiquitously expressed in mammalian tissues, suggesting an important role in choline transportation. Excluding the prospect that CHT1 and OCT1-3 operate during choline transportation in Fa2N-4 cells, we hypothesize that CTL1 is solely responsible for extracellular choline transportation associated with Fa2N-4 cells. However, it may be that CTL2-5 are also involved in choline transportation in such cells. Nevertheless, because the functional characteristics of CTL2-5 have not been completely investigated, it is difficult to determine their roles in choline transportation. To further support our hypothesis that CTL1 is the primary extracellular choline transporter in Fa2N-4 cells, we examined CTL1 expression and localization. A major band of approximately 70 kDa was observed in the immunoblots of Fa2N-4 cell-derived proteins, which corresponded with the estimated size of human CTL1 of 73.3 kDa. Immunofluorescence staining and visualization of CTL1 showed this to overlap with NaK-ATPase, clearly indicating CTL1 expression in the cell membrane. Although we did not directly show a biochemical association of CTL1 with extracellular choline transportation, we sought to support our hypothesis that CTL1 is responsible for choline transportation by investigating [methyl-^{3}H]choline uptake in Fa2N-4 cells. However, because immunofluorescence staining of CTL2 overlapped with COX IV, a known mitochondrial marker, CTL2 was believed to play an essential role in transporting choline to mitochondria in Fa2N-4 cells. Furthermore, choline oxidation occurs in the mitochondria; in particular, it is elevated in the liver and kidneys, corresponding to the high energy demand of hepatocytes (24). Therefore, it follows that choline transporters are abundantly expressed at these locations. Based on mRNA expression analysis, western blot analysis and immunofluorescence staining, we hypothesized that CTL2 may be responsible for choline transportation in the mitochondria. However, we cannot eliminate the possibility that a novel, yet unidentified transporter, distinct from CTL2, has a function in choline transportation in the mitochondria. Moreover, our hypothesis is only based on mRNA and protein expression analysis. Further functional studies are necessary to draw a conclusion on a role for CTL2 in choline transportation in the mitochondria.

Next, we assessed the effects of choline deficiency and the inhibition of choline uptake on Fa2N-4 cells. Because the two treatments reduced cell viability, upregulated caspase-3 and -7 activities and markedly increased FITC-Annexin V immunofluorescence staining, we attributed these changes to apoptosis. Previous reports have described how choline deficiency or the inhibition of choline uptake induced apoptosis via the p53 pathway by increasing the synthesis of ceramide, a known apoptosis-inducing substance (25). Sphingomyelin, a principal component of the cell membrane, can be separated into ceramide and phosphorylcholine by sphingomyelinase (PC); consequently, PC can be used as a donor in phospholipid synthesis (9). In addition, PC after hydrolysis mediates Raf activation in response to mitogenic growth factors (26). These mechanisms indicate that the choline transportation system, via CTL1, is well associated with cell survival.

Next, we explored the modulation of choline uptake via CTL1. PKC operates as one of the key signals in modulating the trafficking of transporters to the cell membrane, e.g., GABA transporter (27), serotonin transporter (28), dopamine transporter, and excitatory amino acid carrier (28,29). Except in trafficking, neuronal PKC activity can regulate CHT1 protein and its surface expression, suggesting that CHT is a phosphoprotein (30). CTL1 modulation and trafficking by PKC signaling have been reported in human THP-1 monocytic cells, while PMA treatment has been demonstrated to induce impaired CTL1 trafficking at the plasma membrane level and to inhibit choline transportation (7). However, it was concluded that PMA treatment induced THP-1 monocytic cell differentiation in macrophages, resulting in altered choline uptake. In the current study, we used Fa2N-4, an established immortalized human hepatocyte cell line that has proven to be useful for liver-based *in vitro* testing and liver research (31,32). Regarding the PKC-dependent pathway in Fa2N-4 cells, treatment with palmitic acid has been associated with PKC signaling and has led to the induction of CYP3A4 activity (33). However, investigations regarding the effect of PKC signaling on CTL1 modulation and trafficking in Fa2N-4 or HepG2 cells are lacking. PKC is a known key regulator of cell growth, and its hyperactivation is believed to play a major role in tumor progression (34). Because the HepG2 cell line is derived from a hepatoblastoma, the expectation was that its progression would be easily affected by PKC stimulation (35). Therefore, we selected the Fa2N-4 cell line for this study. We showed a proportional increase of choline uptake by Fa2N-4 cells with increasing PMA concentrations and also showed that PKC stimulation induced CTL1 translocation into the cell membrane. Accordingly, we conclude that PKC stimulation induced CTL1 to translocate to the cell membrane, resulting in improved choline uptake. However, our study was limited in that we only investigated whether PMA treatment resulted in changes in choline uptake and did not consider the possibility that such changes also reflect the total outcome of PKC-dependent functions. Moreover, it is known that PKC delivers insulin signals at the same time, and that the hyperinsulinemia state is considerably associated with non-alcoholic fatty liver disease (NAFLD). However, we did not examine the pathological role of the CTL1/PKC axis in hyperinsulinemia in this current study. We intend to explore this relationship in future. To dissect the phenomenon of PKC signaling overall, it is necessary to examine the role of each PKC phosphorylation site of CTL1 in the choline uptake system.

We believe that the current investigation on the choline uptake system in human immortalized hepatic cells will help in providing a fundamental understanding of its contribution to the pathogenesis of hepatic diseases. For instance, choline deficiency in non-alcoholic steatohepatitis (NASH) model mice

induces fat accumulation and hepatic inflammation, leading to fatty liver disease. The mechanism underlying this disease is associated with PKC activation (36,37). Moreover, it is known that despite the availability of sufficient choline, inhibition of phosphatidylethanolamine methyltransferase leads to the pathogenesis of lean NASH (38). Exogenous choline deficiency has been shown to be related to the pathogenesis of NAFLD, NASH, and hepatocarcinogenesis (10-12). Therefore, it is obvious that choline is essential for liver homeostasis, and that a higher dietary choline intake is associated with a lower risk of NAFLD and primary liver cancer (39,40). Then, the current study placed one of major focuses on lean state conditions by inducing choline shortage to Fa2N-4 cells. It is logical that researchers have focused on, or are likely to focus on, the metabolites of choline and its related enzymes. Primarily, considering the pathogeneses of NAFLD and NASH, choline uptake via CTL1 may be limited in hepatocytes. It has been demonstrated that patients with NAFLD and NASH have lower accumulated choline in the liver on positron emission tomography-computed tomography (41). However, regarding the pathogenesis of hepatocellular carcinoma (HCC) and lean NASH being induced under choline-deficient conditions, we believe that a possible mechanism is that a choline-deficient condition causes an increase in ceramide concentration via sphingomyelin activation, consequently inducing cell damage and apoptosis. Hence, we believe that exploring the modulation of the choline uptake system via CTL1 by PKC signaling may provide a novel strategy to treat NAFLD, NASH, and HCC in future.

Although we present novel findings that facilitate our understanding of hepatic choline transportation, the major limitation of this study is that *in vitro* only studies were undertaken. In addition, we did not examine whether PKC directly regulates CTL1 to translocate to the cell membrane and induce increased extracellular choline uptake, or whether this occurred by phosphorylation signals to CTL1 proteins. It is necessary to explore these relationships in future. Moreover, it is imperative to further investigate our hypothesis using *in vivo* conditions and clinical trials to gain a better understanding of hepatic disorders, such as NAFLD, NASH, and HCC.

In summary, we conclude that extracellular choline is transported via CTL1 in Fa2N-4 cells. Moreover, we hypothesize that CTL1 and the choline uptake system are associated with cell survival, and that the choline uptake system is modulated by PKC signaling via increased cell surface CTL1 expression. These findings may provide further insights into the pathogenesis of liver disease.

Acknowledgements

Not applicable.

Funding

No funding was received.

Authors' contributions

TI, MO and MI made substantial contributions to the conception of the present study. TI and MI performed the experiments, analyzed and interpreted the data. TI was involved in writing and revising the manuscript and MI assisted with writing and revising the manuscript. HS, JS and RS assisted with the analysis, interpretation of data and revised the manuscript critically. TY was involved in the experimental work and reviewed the manuscript critically. RS, MO and MI supervised the research. All authors read and approved the final version of the manuscript. All authors agreed to be accountable for all aspects of the work in ensuring that questions related to the accuracy or integrity of the work are appropriately investigated and resolved.

Availability of data and materials

The datasets used and/or analyzed during the current study are available from the corresponding author on reasonable request.

Ethics approval and consent to participate

Not applicable.

Patient consent for publication

Not applicable.

Competing interests

The authors declare that they have no competing interests.

References

1. Michel V, Yuan Z, Ramsubir S and Bakovic M: Choline transport for phospholipid synthesis. Exp Biol Med (Maywood) 231: 490-504, 2006.
2. Okuda T, Haga T, Kanai Y, Endou H, Ishihara T and Katsura I: Identification and characterization of the high-affinity choline transporter. Nat Neurosci 3: 120-125, 2000.
3. Koepsell H, Lips K and Volk C: Polyspecific organic cation transporters: Structure, function, physiological roles, and biopharmaceutical implications. Pharm Res 24: 1227-1251, 2007.
4. Traiffort E, Ruat M, O'Regan S and Meunier FM: Molecular characterization of the family of choline transporter-like proteins and their splice variants. J Neurochem 92: 1116-1125, 2005.
5. Nakamura T, Fujiwara R, Ishiguro N, Oyabu M, Nakanishi T, Shirasaka Y, Maeda T and Tamai I: Involvement of choline transporter-like proteins, CTL1 and CTL2, in glucocorticoid-induced acceleration of phosphatidylcholine synthesis via increased choline uptake. Biol Pharm Bull 33: 691-696, 2010.
6. Robinson MB: Regulated trafficking of neurotransmitter transporters: Common notes but different melodies. J Neurochem 80: 1-11, 2002.
7. Fullerton MD, Wagner L, Yuan Z and Bakovic M: Impaired trafficking of choline transporter-like protein-1 at the plasma membrane and inhibition of choline transport in THP-1 monocyte-derived macrophages. Am J Physiol Cell Physiol 290: C1230-C1238, 2006.
8. Schenkel LC, Sivanesan S, Zhang J, Wuyts B, Taylor A, Verbrugghe A and Bakovic M: Choline supplementation restores substrate balance and alleviates complications of Pcyt2 deficiency. J Nutr Biochem 26: 1221-1234, 2015.
9. Michel V and Bakovic M: The ubiquitous choline transporter SLC44A1. Cent Nerv Syst Agents Med Chem 12: 70-81, 2012.
10. Butler LM, Arning E, Wang R, Bottiglieri T, Govindarajan S, Gao YT and Yuan JM: Prediagnostic levels of serum one-carbon metabolites and risk of hepatocellular carcinoma. Cancer Epidemiol Biomarkers Prev 22: 1884-1893, 2013.
11. Ghoshal AK and Farber E: The induction of liver cancer by dietary deficiency of choline and methionine without added carcinogens. Carcinogenesis 5: 1367-1370, 1984.

12. Rinella ME, Elias MS, Smolak RR, Fu T, Borensztajn J and Green RM: Mechanisms of hepatic steatosis in mice fed a lipogenic methionine choline-deficient diet. J Lipid Res 49: 1068-1076, 2008.
13. Nishiyama R, Nagashima F, Iwao B, Kawai Y, Inoue K, Midori A, Yamanaka T, Uchino H and Inazu M: Identification and functional analysis of choline transporter in tongue cancer: A novel molecular target for tongue cancer therapy. J Pharmacol Sci 131: 101-109, 2016.
14. Haubrich DR and Gerber NH: Choline dehydrogenase. Assay, properties and inhibitors. Biochem Pharmacol 30: 2993-3000, 1981.
15. Wiedeman AM, Dyer RA, Green TJ, Xu Z, Barr SI, Innis SM and Kitts DD: Variations in plasma choline and metabolite concentrations in healthy adults. Clin Biochem 60: 77-83, 2018.
16. Apparsundaram S, Ferguson SM, George AL Jr and Blakely RD: Molecular cloning of a human, hemicholinium-3-sensitive choline transporter. Biochem Biophys Res Commun 276: 862-867, 2000.
17. Burckhardt G and Wolff NA: Structure of renal organic anion and cation transporters. Am J Physiol Renal Physiol 278: F853-F866, 2000.
18. Gründemann D, Liebich G, Kiefer N, Köster S and Schömig E: Selective substrates for non-neuronal monoamine transporters. Mol Pharmacol 56: 1-10, 1999.
19. Kouji H, Inazu M, Yamada T, Tajima H, Aoki T and Matsumiya T: Molecular and functional characterization of choline transporter in human colon carcinoma HT-29 cells. Arch Biochem Biophys 483: 90-98, 2009.
20. Uchida Y, Inazu M, Takeda H, Yamada T, Tajima H and Matsumiya T: Expression and functional characterization of choline transporter in human keratinocytes. J Pharmacol Sci 109: 102-109, 2009.
21. Nagashima F, Nishiyama R, Iwao B, Kawai Y, Ishii C, Yamanaka T, Uchino H and Inazu M: Molecular and functional characterization of choline transporter-like proteins in esophageal cancer cells and potential therapeutic targets. Biomol Ther 26: 399-408, 2018.
22. Inazu M, Yamada T, Kubota N and Yamanaka T: Functional expression of choline transporter-like protein 1 (CTL1) in small cell lung carcinoma cells: A target molecule for lung cancer therapy. Pharmacol Res 76: 119-131, 2013.
23. Yara M, Iwao B, Hara N, Yamanaka T, Uchino H and Inazu M: Molecular and functional characterization of choline transporter in the human trophoblastic cell line JEG-3 cells. Placenta 36: 631-637, 2015.
24. Kaplan CP, Porter RK and Brand MD: The choline transporter is the major site of control of choline oxidation in isolated rat liver mitochondria. FEBS Lett 321: 24-26, 1993.
25. Zhang XH, Zhao C and Ma ZA: The increase of cell-membranous phosphatidylcholines containing polyunsaturated fatty acid residues induces phosphorylation of p53 through activation of ATR. J Cell Sci 120: 4134-4143, 2007.
26. Cai H, Erhardt P, Troppmair J, Diaz-Meco MT, Sithanandam G, Rapp UR, Moscat J and Cooper GM: Hydrolysis of phosphatidylcholine couples Ras to activation of Raf protein kinase during mitogenic signal transduction. Mol Cell Biol 13: 7645-7651, 1993.
27. Beckman ML, Bernstein EM and Quick MW: Multiple G protein-coupled receptors initiate protein kinase C redistribution of GABA transporters in hippocampal neurons. J Neurosci 19: RC9, 1999.
28. Jayanthi LD, Samuvel DJ, Blakely RD and Ramamoorthy S: Evidence for biphasic effects of protein kinase C on serotonin transporter function, endocytosis, and phosphorylation. Mol Pharmacol 67: 2077-2087, 2005.
29. Daniels GM and Amara SG: Regulated trafficking of the human dopamine transporter. Clathrin-mediated internalization and lysosomal degradation in response to phorbol esters. J Biol Chem 274: 35794-35801, 1999.
30. Gates J Jr, Ferguson SM, Blakely RD and Apparsundaram S: Regulation of choline transporter surface expression and phosphorylation by protein kinase C and protein phosphatase 1/2A. J Pharmacol Exp Therap 310: 536-545, 2004.
31. Hariparsad N, Carr BA, Evers R and Chu X: Comparison of immortalized Fa2N-4 cells and human hepatocytes as in vitro models for cytochrome P450 induction. Drug Metab Dispos 36: 1046-1055, 2008.
32. Ramboer E, Vanhaecke T, Rogiers V and Vinken M: Immortalized human hepatic cell lines for in vitro testing and research purposes. Methods Mol Biol 1250: 53-76, 2015.
33. Hu N, Hu M, Duan R, Liu C, Guo H, Zhang M, Yu Y, Wang X, Liu L and Liu X: Increased levels of fatty acids contributed to induction of hepatic CYP3A4 activity induced by diabetes-in vitro evidence from HepG2 cell and Fa2N-4 cell lines. J Pharmacol Sci 124: 433-444, 2014.
34. Rumsby M, Schmitt J, Sharrard M, Rodrigues G, Stower M and Maitland N: Human prostate cell lines from normal and tumourigenic epithelia differ in the pattern and control of choline lipid headgroups released into the medium on stimulation of protein kinase C. Br J Cancer 104: 673-684, 2011.
35. Bouma ME, Rogier E, Verthier N, Labarre C and Feldmann G: Further cellular investigation of the human hepatoblastoma-derived cell line HepG2: Morphology and immunocytochemical studies of hepatic-secreted proteins. In Vitro Cell Dev Bio 25: 267-275, 1989.
36. Greene MW, Burrington CM, Lynch DT, Davenport SK, Johnson AK, Horsman MJ, Chowdhry S, Zhang J, Sparks JD and Tirrell PC: Lipid metabolism, oxidative stress and cell death are regulated by PKC delta in a dietary model of nonalcoholic steatohepatitis. PLoS One 9: e85848, 2014.
37. Greene MW, Burrington CM, Ruhoff MS, Johnson AK, Chongkrairatanakul T and Kangwanpornsiri A: PKC{delta} is activated in a dietary model of steatohepatitis and regulates endoplasmic reticulum stress and cell death. J Biol Chem 285: 42115-42129, 2010.
38. Nakatsuka A, Matsuyama M, Yamaguchi S, Katayama A, Eguchi J, Murakami K, Tesgigawara S, Ogawa D, Wada N, Yasunaka T, *et al*: Insufficiency of phosphatidylethanolamine N-methyltransferase is a risk for lean non-alcoholic steatohepatitis. Sci Rep 6: 21721, 2016.
39. Yu D, Shu XO, Xiang YB, Li H, Yang G, Gao YT, Zheng W and Zhang X: Higher dietary choline intake is associated with lower risk of nonalcoholic fatty liver in normal-weight Chinese women. J Nutr 144: 2034-2040, 2014.
40. Zhou RF, Chen XL, Zhou ZG, Zhang YJ, Lan QY, Liao GC, Chen YM and Zhu HL: Higher dietary intakes of choline and betaine are associated with a lower risk of primary liver cancer: A case-control study. Sci Rep 7: 679, 2017.
41. Roppongi M, Izumisawa M, Terasaki K, Muraki Y and Shozushima M: ^{18}F-FDG and ^{11}C-choline uptake in proliferating tumor cells is dependent on the cell cycle in vitro. Ann Nucl Med 33: 237-243, 2018.